Molecular Crystals and Liquid Crystals

ISSN: 1542-1406 (Print) 1563-5287 (Online) Journal homepage: http://www.tandfonline.com/loi/gmcl20

Electroluminescent properties of naphthalene end-capping bis-anthracene derivatives

Se Hyun Kim, Jwajin Kim, Song Eun Lee, Young Kwan Kim & Seung Soo Yoon

To cite this article: Se Hyun Kim, Jwajin Kim, Song Eun Lee, Young Kwan Kim & Seung Soo Yoon (2016) Electroluminescent properties of naphthalene end-capping bis-anthracene derivatives, Molecular Crystals and Liquid Crystals, 636:1, 30-37, DOI: 10.1080/15421406.2016.1200940

To link to this article: http://dx.doi.org/10.1080/15421406.2016.1200940

Published online: 01 Nov 2016.

MOLECULAR CRYSTALS AND LIQUID CRYSTALS
2016, VOL. 636, 30–37
http://dx.doi.org/10.1080/15421406.2016.1200940

Taylor & Francis
Taylor & Francis Group

Electroluminescent properties of naphthalene end-capping bis-anthracene derivatives

Se Hyun Kim[a], Jwajin Kim[a], Song Eun Lee[b], Young Kwan Kim[b], and Seung Soo Yoon[a]

[a]Department of Chemistry, Sungkyunkwan University, Suwon, Korea; [b]Department of Information Display, Hongik University, Seoul Korea

ABSTRACT

We designed naphthalene moieties end-capping bis-anthracene derivatives and characterized their photophysical properties. We fabricated two set of devices with the structure of ITO /2-TNATA (60 nm) /NPB (10 nm) /emitter (**1–3**) (40 nm) /Alq_3 (15 nm) /Liq (2 nm) /Al for devices **1B–3B** and same structure without 2-TNATA for **1A–3A**. A device using 2-TNATA exhibited luminous efficiency of 5.98 cd/A, power efficiency of 3.09 lm/W and external quantum efficiency of 3.49% at 200 cd/m^2, respectively, while a same device without 2-TNATA layer showed 3.52 cd/A, 1.79 lm/W, and 2.22% at 200 cd/m^2, respectively.

KEYWORDS

Organic light-emitting diode; Bis-anthracene derivatives; Hole injection layer; Electromer

Introduction

OLEDs have attracted much attention due to their potential applications in full-color flat panel displays, and solid-state lighting [1]. Over the past years, many researchers have focused on the development of the efficient OLEDs with high quantum yields and good thermal stabilities [2–6]. Particularly, much interest has been focused on anthracene derivatives due to its wide-energy bandgap, high quantum yield, and good thermal stability. Among those 9,10-diphenylanthracene (DPA) is a good candidate for blue emitting material because of excellent fluorescent quantum yield in solution [7]. However, an anthracene moieties with the planar structure has strong close-packing and excimer formation, which lead to the decrease of electroluminescent efficiencies and color purity [8].

To resolve this problem, 1,4-bis(9-(2-naphthyl)anthracene-10-yl)benzene had been designed for reducing the intermolecular interaction and preventing the self-aggregation in our previous research and it showed the high luminous efficiency (LE), power efficiency (PE), and external quantum efficiency (EQE) of 3.52 cd/A, 1.79 lm/W, and 2.22% at 200 cd/m^2 in non-doped system [9].

We synthesized emitters **1–3** based on bis-anthracenylphenylenes end-capped with naphthalene groups; 1,4-bis(9-(1-naphthyl)anthracene-10-yl)benzene (**1**) [10], 4,4′-bis(9-(1-naphthyl)anthracene-10-yl)biphenyl (**2**) [11], 1,4-bis(9-(2-naphthyl)anthracene-10-yl)benzene (**3**) [10]. In these materials **1–3**, anthracene moieties as well as the end-capped naphthyl group would induce the non-planar structural features in **1–3**. Consequently, these

CONTACT Seung Soo Yoon ssyoon@skku.edu Department of Chemistry, Sungkyunkwan University, 300, Cheoncheon-dong, Jangan-gu, Suwon, Gyeonggi-do, Korea; Young Kwan Kim kimyk@hongik.ac.kr Department of Information Display, Hongik University, 72-1, Sangsu-dong, Mapo-gu, Seoul, Korea.

Color versions of one or more of the figures in the article can be found online at www.tandfonline.com/gmcl.

non-planar structural properties of **1**–**3** would lead to the improved EL efficiencies of devices using them by preventing the intermolecular interaction and the self-aggregation between materials **1**-**3** in solid state devices.

To further increase electroluminescent (EL) efficiencies in OLEDs, it needs to control injection and transportation of holes and electrons in OLED devices. Therefore, the optimization of device structure is of great importance. 2-TNATA (4,4′,4″-tris(N-(2-naphthyl)-N-phenylamino)-triphenylamine) is π-electron starburst molecule with the suitable energy levels for the hole injection layer (HIL). In this study, 2-TNATA is placed as an interlayer between indium tin oxide (ITO) anode and NPB as the HIL in OLEDs using **1**–**3** as the emitting materials. As will be seen in below, the enhancement of the hole injection in OLED's including 2-TNATA as the HIL leads to the higher efficiencies than those without 2-TNATA layer.

Experimental

Physical measurements

The UV-vis absorption and photoluminescence spectra of **1**–**3** were measured in dichloromethane (10^{-5} M) using Shimadzu UV-1650PC and Aminco-Browman series 2 luminescence spectrometers. The fluorescence quantum yields of the emitting materials were determined in dichloromethane at 293 K using DPA (9,10-diphenylanthracene) as a reference ($\Phi_{DPA} = 0.86$) [7]. The values of relative fluorescence quantum yield were acquired using the formula explained $\Phi_X = \Phi_{DPA}$ ($Grad_X/Grad_{DPA}$)($\eta^2{}_X/\ \eta^2{}_{DPA}$). The HOMO (highest occupied molecular orbital) energy levels were measured with a low-energy photoelectron spectrometer (Riken-Keiki, AC-2). The energy band gaps were determined from the intersection of the absorption and photoluminescence spectra. The LUMO (lowest unoccupied molecular orbital) energy levels were calculated by subtracting the corresponding optical band gap energies from the HOMO energy values.

OLED fabrication and measurement

For fabricating OLEDs, ITO thin films coated on glass substrates were used, which was 30 square of the sheet resistivity, and 100 nm of thickness. The ITO-coated glass was cleaned in an ultrasonic bath by the following sequence: acetone, methyl alcohol, distilled water, and stored in isopropyl alcohol for 48 h and dried by a N_2 gas gun. The substrates were treated by O_2 plasma under 2.0×10^{-2} torr at 125 W for 2 min. All organic materials and metals were deposited under high vacuum (5×10^{-7} torr).

The current density (J), luminance (L), luminous efficiency (LE), power efficiency (PE), external quantum efficiency (EQE), and CIE chromaticity coordinates of the OLEDs were measured with a Keithley 2400, Chroma meter CS-1000A. Electroluminance was measured using a Roper Scientific Pro 300i.

Results and discussion

The molecular structures of the designed blue fluorescent materials **1**–**3** are shown in Scheme 1. Figure 1 shows the UV-vis absorption and photoluminescence (PL) spectra of fluorescence emitting materials **1**–**3** in dichloromethane solutions and solid state on quartz plate films. Optical properties of **1**–**3** are summarized in Table 1. As shown in the absorption

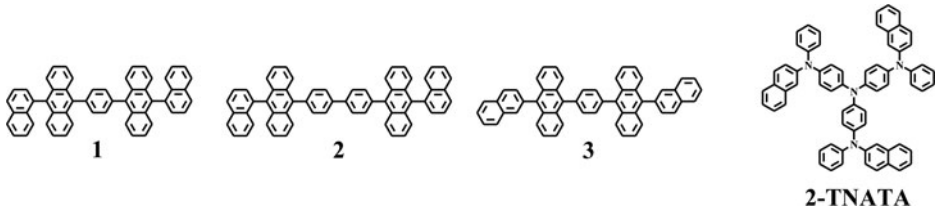

Scheme 1. Structures of compounds (**1**–**3**) and 2-TNATA as HIL.

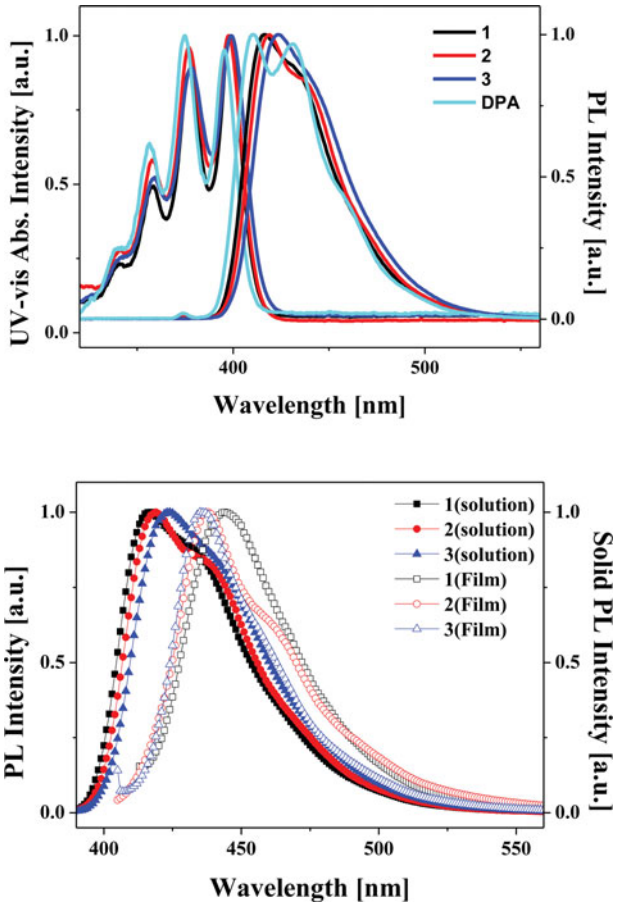

Figure 1. The absorption spectra, emission spectra in solution and emission spectra in thin film state of emitting materials (**1**–**3**).

Table 1. Optical properties of compounds (**1**–**3**).

Compound	UV_{max} [a] [nm]	PL_{max} [a] [nm]	PL_{max} [b] [nm]	FWHM[a] [nm]	HOMO/ LUMO [eV]	E_g [eV]	Φ[c] [%]
1	398	417	444	50	−5.82 / −2.76	3.06	0.84
2	377	419	438	49	−5.88 / −2.83	3.05	0.77
3	399	424	435	51	−5.80 / −2.77	3.03	0.80

[a.] CH_2Cl_2 solution (10^{-5} M). [b.]Thin film. [c.]Using DPA (9,10-diphenylanthracene) as a standard; $\lambda_{ex} = 360$ nm ($\Phi = 0.86$ in CH_2Cl_2).

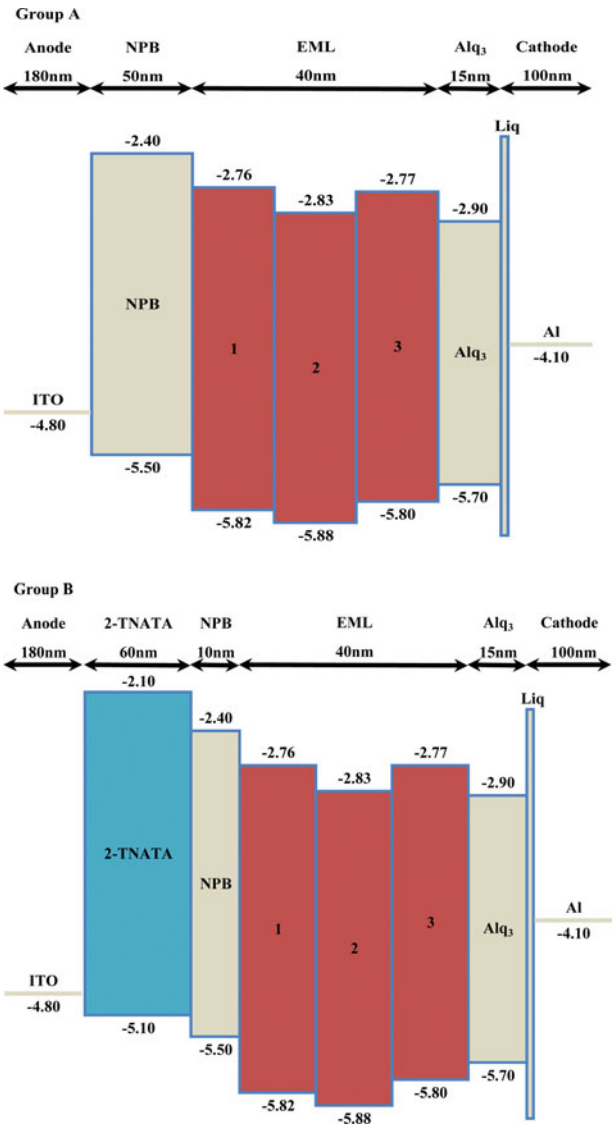

Figure 2. Energy levels diagram of compounds (**1**–**3**) used in the OLED fabrication.

spectra, the maximum absorption wavelengths of **1**–**3** shown at 398, 377, and 399 nm that represented the characteristic vibrational pattern of the isolated anthracene group. Also, the maximum emission wavelengths of **1**–**3** showed at 417, 419, and 424 nm in solution. Solid state PL spectra of **1**–**3** are shifted to red region rather than solution PL spectra (ca. 11–27 nm) due to the solid state effect. The HOMO energy levels of **1**–**3** measured by a photoelectron spectrometer (Riken-Keiki AC-2) are −5.82, −5.88, and −5.80 eV, respectively. The LUMO energy levels of **1**–**3** calculated from their E_g values and the LUMO energy levels of **1**–**3** are −2.76, −2.83, and −2.77 eV, respectively.

To evaluate electroluminescent properties of compounds **1**–**3**, devices **1A**–**3A** with configuration: ITO /4,4′-Bis(*N*-(1-naphthyl)-*N*-phenylamino)biphenyl (NPB) (50 nm) /emitter (**1**–**3**) (40 nm) /Tris(8-hydroxyquinolinato)aluminium (Alq_3) (15 nm) /Lithium quinolate (Liq) (2 nm) /Al (100 nm) were fabricated, respectively. Figure 2 shows the energy level diagrams of devices using compounds **1**–**3**. EL spectra of devices **1A**–**3B** are shown in Figure 3.

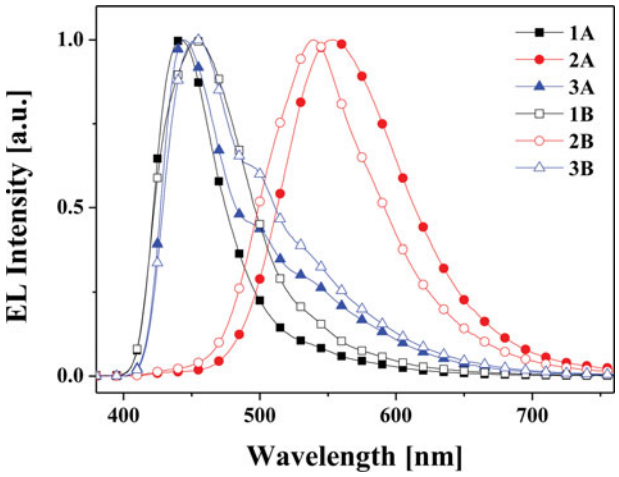

Figure 3. EL spectra of the devices (**1A**–**3B**).

Devices **1A** and **3A** exhibited deep-blue emission with the maximum peaks at 442 and 444 nm, respectively, which were similar to the solid state PL spectra of the emitters **1** and **3**. The CIE coordinates of Devices **1A** and **3A** were (0.163, 0.096) and (0.197, 0.197), respectively, at 8.5 V. However, device **2A** exhibits mainly the greenish emission at 553 nm with the CIE coordinates of (0.412, 0.541). EL spectrum of device **2A** differs significantly from solid state PL spectra of the emitter **2** in device **2A**. This interesting feature normally observed due to the electromer or electroplex [12]. The existence of the electromer or electroplex caused by relatively high electric fields usually leads to a red-shifted and broadened emission spectrum [13].

To investigate the efficiency differences originated from the presence of a hole injection layer of OLEDs, devices **1B**–**3B** with configuration: ITO /2-TNATA (60 nm) /NPB (10 nm)/ Emitting materials (**1**–**3**) (40 nm) /Alq_3 (15 nm) /Liq (2 nm) /Al were fabricated, respectively. In these devises, ITO(indium-tin-oxide) and Liq:Al are the anode and the cathode, respectively, and 4,4′,4″-tris(*N*-(2-naphthyl)-*N*-phenyl-amino)triphenylamine (2-TNATA) is used as the hole injection layer (HIL).

EL spectra of devices **1B**–**3B** exhibited the similar trends to those of devices **1A**–**3A**, respectively. For examples, devices **1B** and **3B** showed the emission from singlet exciton of the emitters **1** and **3**, respectively. Also, device **2B** exhibited the emission from the electromer or electroplex of the emitter **2**.

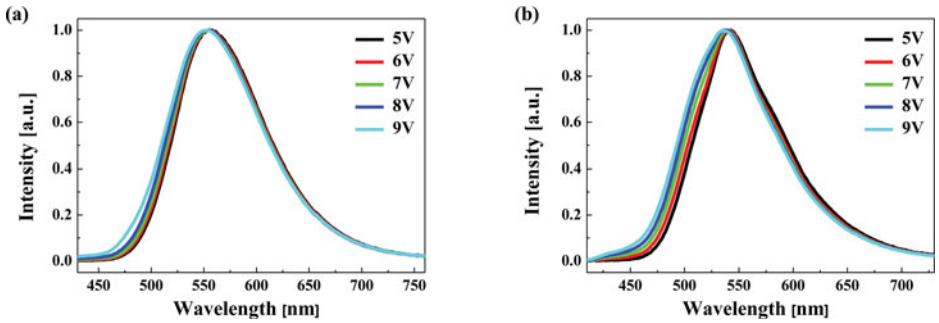

Figure 4. EL spectra of the devices (a) **2A** and (b) **2B** measured at different voltage.

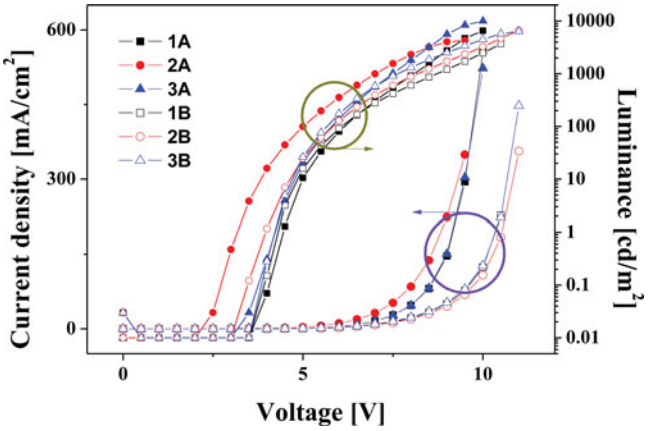

Figure 5. Current density-Voltage (*J-V*) and Luminance-Voltage (*L-V*) curves of the devices (**1A**–**3B**).

Figure 4 is EL spectra measured at different voltage of the devices **2A** and **2B**. Compared with devices **2A** and **2B**, the EL spectra of the other devices **1A**, **3A**, **1B**, and **3B** are showed little differences. However, EL spectra of device **2B** changed largely depending on voltage. EL spectra of devices **2A** and **2B** that generated from electromer or electroplex of the emitter **2** are more sensitive to electric field than other devices. These observations imply that electromers or electroplexs are affected by strength of electric fields severely.

Figure 5 shows current density-voltage-luminance (*J-V-L*) characteristics of the devices **1A**–**3B**. Table 2 summarizes *J-V-L* characteristics and EL efficiencies of devices **1A**–**3B**.

The luminous efficiencies (LE), power efficiencies (PE), and external quantum efficiencies (EQE) of devices **1A**–**3B** as a function of the luminance are shown in Figure 6. Compared to the devices **1A**–**3A** without 2-TNATA layer as HIL layer, devices **1B**–**3B** with 2-TNATA exhibited the improved EL efficiencies. For example, by using 2-TNATA as the hole injection layer (HIL), the external quantum efficiencies of OLEDs using emitting materials **1**–**3** were increased by 28, 53, and 57% at 200 cd/m^2, respectively. Because the HOMO levels of the NPB and 2-TNATA are −5.5 and −5.1 eV, respectively, the device with 2-TNATA lowers the hole injection barrier to the emitting layer. This would contribute to the higher EL efficiencies in the device fabricated with 2-TNATA.

Table 2. EL efficiencies and CIE coordinates of devices using compounds **1**–**3**.

Device	λ_{max}[a] / FWHM [nm]	J[b] [mA/cm^2]	L[b] [cd/m^2]	LE[a/c] [cd/A]	PE[a/c] [lm/W]	EQE[a/c] [%]	CIE[d] (x, y)
1A	442 / 53	294	4674	1.97 / 1.95	1.27 / 0.93	2.20 / 2.05	(0.163, 0.096)
2A	553 / 101	349	4295	3.32 / 3.32	2.49 / 1.90	1.05 / 1.05	(0.412, 0.541)
3A	444 / 55	303	8383	3.86 / 3.52	2.02 / 1.79	2.42 / 2.22	(0.197, 0.197)
1B	454 / 74	76	1717	3.16 / 3.15	1.71 / 1.49	2.62 / 2.61	(0.162, 0.139)
2B	540 / 92	69	2350	5.25 / 5.24	3.09 / 2.60	1.61 / 1.61	(0.342, 0.550)
3B	454 / 82	80	3393	6.29 / 5.98	3.11 / 3.09	3.68 / 3.49	(0.196, 0.221)

[a.] Maximum value. [b.]Value measured at 9.5 V. [c.]Value measured at 200 cd/m^2. [d.]Value measured at 8.5 V.

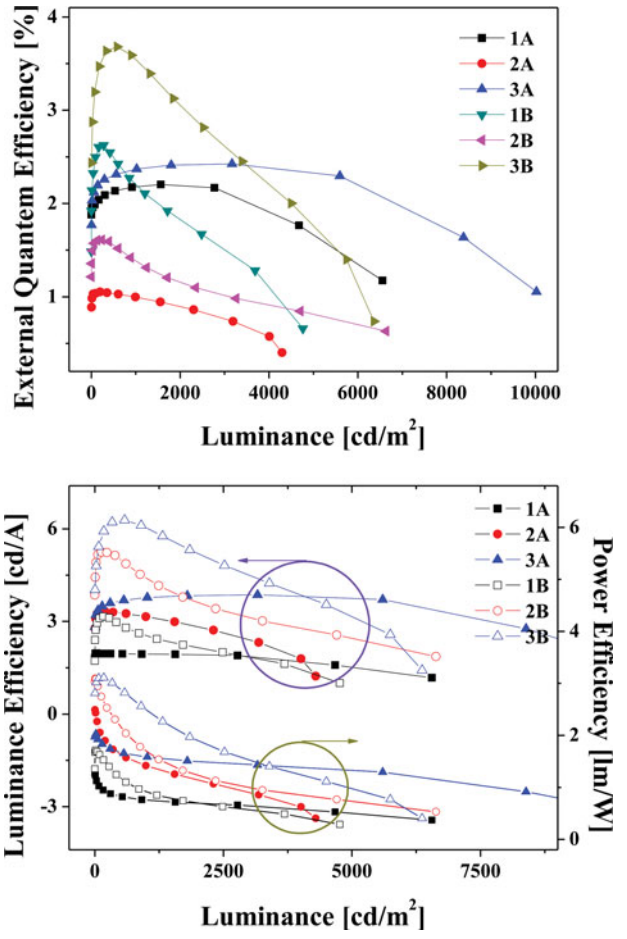

Figure 6. Luminous efficiencies, power efficiencies, and external quantum efficiencies as a function of luminance for the devices (**1A**–**3B**).

Conclusions

We fabricated two set of devices with the structure of ITO /2-TNATA (60 nm) /NPB (10 nm) /emitter (**1**–**3**) (40 nm) /Alq_3 (15 nm) /Liq (2 nm) /Al for devices **1B**–**3B** and same structure without 2-TNATA for **1A**–**3A**. Compared to devices **1A**–**3A**, the EL performances of OLED devices **1B**–**3B** were significantly increased due to the improved hole injection ability through 2-TNATA. By using 2-TNATA as the HIL, a highly efficient blue OLED with the external quantum efficiency of 3.49% at 200 cd/m^2 was developed.

Acknowledgments

This research was supported by the Samsung Display and Basic Science Research Program through the NRF funded by the Ministry of Education, Science and Technology, South Korea (NRF-2013R1A1A2A10008105).

References

[1] Tang, C. W., & Vanslyke, S. A. (1987). *Appl. Phys. Lett.*, *51*, 51913.

[2] Lee, K. H., Son, C. S., Lee, J. Y., Kang, S., Yook, K.S., Jeon, S. O., Lee, J. Y., & Yoon, S. S. (2011). *Eur. J. Org. Chem.*, *25*, 4788.
[3] Lee, K. H., Park, J. K., Seo, J. H., Park, S. W., Kim, Y. S., Kim, Y. K., & Yoon, S. S. (2011). *J. Mater. Chem.*, *21*, 13640.
[4] Lee, K. H., Kwon, Y. S., Lee, J. Y., Kang, S., Yook, K. S., Jeon, S. O., Lee, J. Y., & Yoon, S. S. (2011). *Eur. J. Org. Chem.*, *17*, 12994.
[5] Lee, K. H., Kim, S. O., You, J. N., Kang, S., Lee, J. Y., Yook, K. S., Jeon, S. O., Lee, J. Y., & Yoon, S. S. (2012). *J. Mater. Chem.*, *22*, 5142.
[6] Lee, K. H., Kim, S. O., Kang, S., Lee, J. Y., Yook, K. S., Lee, J. Y., & Yoon, S. S. (2012). *Eur. J. Org. Chem.*, *14*, 2748.
[7] Wu, C. L., Chang, C. H., Chang, Y. T., Chen, C. T., Chen, C. T., and Su, C. J. (2014). *J. Mater. Chem. C.*, *2*, 7188.
[8] Shin, H. T., Lin, C. H., Shi, H. H., & Cheng, C. H. (2002). *Adv. Mater.*, *14*, 1409.
[9] Jang, H. S., Lee, K. H., Lee, S. J., Kim, Y. K., & Yoon, S. S. (2012). *Mol. Cryst. Liq. Cryst.*, *563*, 173.
[10] Kim, H. J., Lee, S. E., Lee, S. J., Kim, Y. K., & Yoon, S. S. (2014). *Mol. Cryst. Liq. Cryst.*, *601*, 142.
[11] Wang, L., Wong, W. Y., Lin, M. F., Wong, W. K., Cheah, K. W., Tan, H. L., & Chen, C. H. (2008). *J. Mater. Chem.*, *18*, 4529.
[12] Shirota, Y., Kuwabara, Y., Okuda, D., Okuda, R., Ogawa, H., Inada, H., Wakimoto, T., Nakada, H., Yonemoto, Y., Kawami, S., & Imai, K. (1997). *J. Luminescence.*, *72*, 985.
[13] Nagarajan, N., Prakash, A., Velmurugan, G., Shakti, N., Katiyar, M., Venuvanalingam, P., & Renganathan, R. (2014). *Dyes Pigmants.*, *102*, 180.